One-dimensional Fermi gas with a single impurity in a harmonic trap: Perturbative description of the upper branch

Seyed Ebrahim Gharashi, X. Y. Yin, Yangqian Yan, and D. Blume

One-dimensional Fermi gas with a single impurity in a harmonic trap: Perturbative description of the upper branch

Seyed Ebrahim Gharashi, X. Y. Yin, Yangqian Yan, and D. Blume[1]

[1]*Department of Physics and Astronomy, Washington State University, Pullman, Washington 99164-2814, USA*

(Dated: December 2, 2014)

The transition from "few to many" has recently been probed experimentally in an ultracold harmonically confined one-dimensional lithium gas, in which a single impurity atom interacts with a background gas consisting of one, two, or more identical fermions [A. N. Wenz *et al.*, Science **342**, 457 (2013)]. For repulsive interactions between the background or majority atoms and the impurity, the interaction energy for relatively moderate system sizes was analyzed and found to converge toward the corresponding expression for an infinitely large Fermi gas. Motivated by these experimental results, we apply perturbative techniques to determine the interaction energy for weak and strong coupling strengths and derive approximate descriptions for the interaction energy for repulsive interactions with varying strength between the impurity and the majority atoms and any number of majority atoms.

PACS numbers:

I. INTRODUCTION

One-dimensional Bose and Fermi systems with contact interactions have been studied for many decades now, especially in the regime where the systems obey periodic boundary conditions [1–5]. A large fraction of the eigenstates can be thought of as corresponding to gas-like states. A second subset of eigenstates corresponds to self-bound droplet-like states. These states maintain their bound state character in the absence of periodic boundary conditions, i.e., in free space. In many cases, both the gas-like and droplet-like states can be obtained analytically via the Bethe ansatz. The Bethe ansatz takes advantage of the fact that the zero-range nature of the interactions, combined with the fact that particles in one dimension have to pass through each other to exchange positions, allows one to identify constants of motion. The solutions can then be derived in terms of these constants of motion. A closely related aspect is that a variety of one-dimensional systems with two-body contact interactions are integrable [1, 4].

The solution of the homogeneous system can be applied to one-dimensional systems under spatially varying external confinement via the local density approximation [6–10]. This approximation typically provides a highly accurate description for a large number of particles but not necessarily for a small number of particles. It is thus desirable to derive more accurate descriptions for small one-dimensional systems with two-body delta-function interactions under external confinement. Unfortunately, extensions of the Bethe ansatz to inhomogeneous systems are, in general, not known. This can be understood intuitively by realizing that the relative two-body momentum in inhomogeneous systems is not conserved due to the presence of the spatially varying confinement. Correspondingly, harmonically trapped one-dimensional few-body systems have been treated numerically by various techniques [7, 11–17].

In this work, we apply standard Raleigh-Schrödinger perturbation theory to harmonically confined systems and derive approximate solutions whose accuracy can be improved systematically by considering successively higher orders in the expansion in the small parameter. We focus on one-dimensional Fermi gases with a single impurity under external harmonic confinement. This system is of particular interest since it has been realized experimentally in Jochim's cold atom laboratory [18, 19]. In the experiments, the impurity is a lithium atom that occupies a hyperfine state different from the hyperfine state that the majority atoms occupy. The trapping geometry is highly-elongated and effectively one-dimensional. We will show that our perturbative results enable us to calculate the energy of the upper branch, which has been studied experimentally, with fairly good accuracy for all N over a wide range of coupling strengths. In addition, our results provide bounds on the energies in the weakly- and strongly-interacting regimes. These bounds can, e.g., be used to assess the accuracy of numerical solutions.

The remainder of this paper is organized as follows. Section II introduces the system Hamiltonian and notation. Section III summarizes our perturbative results. The perturbative results are analyzed in Secs. IV and V. Finally, Sec. VI concludes.

II. SYSTEM HAMILTONIAN

We consider a single impurity immersed in a one-dimensional Fermi gas that consists of N identical mass m fermions. The mass of the impurity is equal to that of the majority or background particles. The impurity, with position coordinate z_0, interacts with the majority particles, with position coordinates z_j $(j = 1, \cdots, N)$, through a zero-range two-body potential with strength g,

$$V_{2\mathrm{b}}(z_{j0}) = g\delta(z_j - z_0), \qquad (1)$$

where $z_{j0} = z_j - z_0$. The Hamiltonian H for the harmonically confined $(N, 1)$ system then reads

$$H = \sum_{j=1}^{N} H_{\text{ho}}(z_j) + H_{\text{ho}}(z_0) + \sum_{j=1}^{N} V_{2\text{b}}(z_{j0}), \qquad (2)$$

where the single particle harmonic oscillator Hamiltonian $H_{\text{ho}}(z)$ is given by

$$H_{\text{ho}}(z) = -\frac{\hbar^2}{2m}\frac{\partial^2}{\partial z^2} + \frac{1}{2}m\omega^2 z^2; \qquad (3)$$

here, ω denotes the angular trapping frequency. The delta-function interactions in Eq. (2) can be replaced by a set of boundary conditions on the many-body wave function $\Psi(z_0, z_1, \cdots, z_N)$,

$$\left(\frac{\partial\Psi}{\partial z_{j0}}\bigg|_{z_{j0}\to 0^+} - \frac{\partial\Psi}{\partial z_{j0}}\bigg|_{z_{j0}\to 0^-}\right) = \frac{gm}{\hbar^2}\Psi|_{z_{j0}\to 0}, \quad (4)$$

where the limits $z_{j0} \to 0^+$, $z_{j0} \to 0^-$, and $z_{j0} \to 0$ are taken while keeping the other N coordinates, i.e., $z_1, \cdots, z_{j-1}, z_{j+1}, \cdots, z_N$ and $(z_j + z_0)/2$, fixed.

In the following, we determine the eigenenergies $E(N)$ of the Hamiltonian H for various N. Throughout, we restrict ourselves to the so-called upper branch. This branch can be populated by preparing the system in the non-interacting limit $(g \to 0^+)$ and by then adiabatically first increasing g to large positive values, then continuing across the confinement-induced resonance [20] to infinitely negative g values and finally increasing g to small negative values. Solid, dotted, and dashed lines in Fig. 1(a) show the energy of the upper branch for $N = 1$ [21], 2, and 3 [14, 15, 22], respectively, as a function of $-1/g$. For all N, the energy increases monotonically as a function of increasing $-1/g$. The upper branch corresponds to the ground state of the model Hamiltonian when g is positive but not when g is negative. For negative g, the model Hamiltonian supports molecular-like bound states. In real cold atom systems, energetically lower-lying molecular states exist even for positive g. However, it has been demonstrated experimentally [19] that the upper branch can be populated with reasonably high fidelity for positive g, motivating us—as well as others [7, 12, 13, 16, 17, 23–26]—to investigate the properties of the upper branch within a stationary zero-temperature quantum mechanics framework. Since decay to states with molecular character can lead to significant depopulation of the upper branch for negative g, our primary focus in the following lies on the positive g portion of the upper branch.

For $g = 0^+$, the energy of the upper branch is equal to $E_{\text{ni}}(N) = (N^2 + 1)\hbar\omega/2$. We write the energy $E(N)$ of the upper branch in terms of the interaction energy $\epsilon(N)$,

$$E(N) = E_{\text{ni}}(N) + \epsilon(N). \qquad (5)$$

Solid, dotted, and dashed lines in Fig. 1(b) show the interaction energies, normalized by the energy $E_{\text{F}}(N)$,
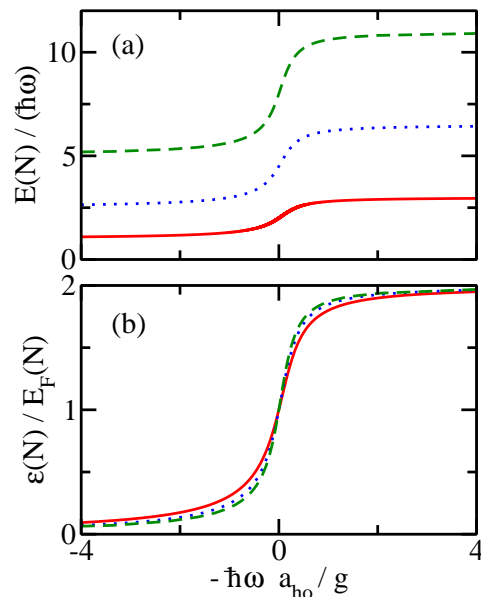

FIG. 1: (Color online) (a) Solid, dotted, and dashed lines show the energy of the upper branch for $N = 1$, 2, and 3 as a function of $-1/g$. The energies of the $(1, 1)$ system are obtained by solving the transcendental equation derived in Ref. [21]. The energies of the $(2, 1)$ and $(3, 1)$ system are taken from Refs. [14, 15, 22]. (b) Solid, dotted, and dashed lines show the interaction energy $\epsilon(N)$, normalized by the Fermi energy $E_{\text{F}}(N)$, for $N = 1$, 2, and 3, respectively, as a function of $-1/g$. The harmonic oscillator length a_{ho} is defined in Eq. (10).

for systems with $N = 1$, 2, and 3 majority particles. The energy $E_{\text{F}}(N)$ is directly proportional to the number of majority particles,

$$E_{\text{F}}(N) = N\hbar\omega. \qquad (6)$$

Figure 1(b) shows that the normalized interaction energy depends relatively weakly on the number of particles. Independent of N, we have $\epsilon(N) = 0$ for $g = 0^+$ and $\epsilon(N) = E_{\text{F}}(N)$ for $|g| = \infty$. As can be read off Figs. 1(a) and 1(b), the energy increase of the upper branch is the same on the positive g side as it is on the negative g side, indicating that $\epsilon(N)$ approaches $2E_{\text{F}}(N)$ in the $g = 0^-$ limit for $N = 1 - 3$. We refer to $E_{\text{F}}(N)$ as the Fermi energy of the majority particles. It should be noted, however, that the "exact" Fermi energy of the majority particles is $E_{\text{F}}(N) - \hbar\omega/2$, i.e., $E_{\text{F}}(N)$ corresponds to the leading order term of the Fermi energy of the majority particles in the large N limit.

One of the main goals of this paper is to derive expansions for the interaction energy of the upper branch around $g = 0^+$ and $|g| = \infty$ using standard Raleigh-Schrödinger perturbation theory for any N, i.e., for $N = 1, \cdots, \infty$. To this end, we express the interaction

energies $\epsilon^{(0^+)}$ and $\epsilon^{(|\infty|)}$ in the vicinity of $g = 0^+$ and $|g| = \infty$, respectively, in a power series of the dimensionless interaction parameter γ (for $|g|$ small) or in a power series of γ^{-1} (for $|g|$ large) [27],

$$\epsilon^{(0^+)}(N) = \left[\sum_{k=1}^{k_{\max}} B^{(k)}(N)\gamma^k\right] E_{\mathrm{F}}(N) + \mathcal{O}(\gamma^{k_{\max}+1}) \quad (7)$$

and

$$\epsilon^{(|\infty|)}(N) =$$
$$\left[1 + \sum_{k=1}^{k_{\max}} C^{(k)}(N)\gamma^{-k}\right] E_{\mathrm{F}}(N) + \mathcal{O}(\gamma^{-(k_{\max}+1)}), \quad (8)$$

where the dimensionless interaction parameter γ is given by

$$\gamma = \frac{\pi}{\sqrt{2N}}\frac{g}{\hbar\omega a_{\mathrm{ho}}}, \quad (9)$$

with

$$a_{\mathrm{ho}} = \sqrt{\frac{\hbar}{m\omega}} \quad (10)$$

denoting the harmonic oscillator length. As we will show below, the scaling of the interaction energy by $E_{\mathrm{F}}(N)$ ensures a smooth connection between the energy shifts for finite and infinite N. In Eqs. (7)-(8), the dimensionless kth-order perturbation theory coefficients $B^{(k)}(N)$ and $C^{(k)}(N)$ depend on N and will be determined in the next section.

III. PERTURBATIVE RESULTS

$N \to \infty$ *limit:* The impurity problem for the homogeneous system with positive γ was solved by McGuire in 1965 [28]. Within the local density approximation the Fermi wave vector is replaced by the wave vector at the trap center such that the interaction energy of the ground state for the harmonically trapped system with $N \to \infty$ becomes [19]

$$\frac{\epsilon(\infty)}{E_{\mathrm{F}}(\infty)} = \frac{\gamma}{\pi^2}\left[1 - \frac{\gamma}{4} + \left(\frac{\gamma}{2\pi} + \frac{2\pi}{\gamma}\right)\arctan\left(\frac{\gamma}{2\pi}\right)\right]. (11)$$

Expanding Eq. (11) around $\gamma = 0^+$ and $|\gamma| = \infty$, respectively, $B^{(k)}(\infty)$ and $C^{(k)}(\infty)$ can be obtained for $k = 1, 2, \cdots$. We find $B^{(1)}(\infty) = 2/\pi^2$, $B^{(2)}(\infty) = -1/(4\pi^2)$, $B^{(3)}(\infty) = 1/(6\pi^4)$, $C^{(1)}(\infty) = -8/3$, $C^{(2)}(\infty) = 0$, and $C^{(3)}(\infty) = 32\pi^2/15$. The numerical values of these coefficients are summarized in Tables I-II. It is readily shown that the small and large γ series, Eqs. (7) and (8), converge for $\gamma < 2\pi$ and $\gamma^{-1} < (2\pi)^{-1}$, respectively. Table II shows that $C^{(2)}(\infty)$ vanishes. We will return to this finding when we discuss the N-dependence of the $C^{(k)}(N)$ coefficients.

TABLE I: Coefficients $B^{(k)}(N)$ for various (N,k) combinations. The numbers in parenthesis denote the uncertainty that arises from evaluating the perturbation theory sums with a finite energy cutoff. The numbers without errorbars have been rounded.

	$k = 1$	$k = 2$	$k = 3$
$N=1$	0.179587	-0.0223551	0.00179230
$N=2$	0.190481	-0.0239838	0.00179523
$N=3$	0.194409	-0.0244852	0.00177603(1)
$N=4$	0.196423	-0.0247210	0.0017627(1)
$N=5$	0.197647	-0.0248563	0.0017535(1)
$N=6$	0.198469	-0.0249435	0.0017470(1)
$N=7$	0.199059	-0.0250042	
$N=8$	0.199503	-0.0250488	
$N=9$	0.199849	-0.0250828	
$N=10$	0.200126	-0.0251096	
$N=11$	0.200353	-0.0251313	
$N=12$	0.200543	-0.0251491	
$N=\infty$	0.202642	-0.0253303	0.00171100

TABLE II: Coefficients $C^{(k)}(N)$ for various (N,k) combinations. The numbers in parenthesis denote the uncertainty that arises from evaluating the perturbation theory sums with a finite energy cutoff. The numbers without errorbars have been rounded.

	$k = 1$	$k = 2$	$k = 3$
$N=1$	-3.54491	3.85603	34.3007
$N=2$	-3.17245	2.41904(1)	25.38(2)
$N=3$	-3.02854	1.8142(2)	23.78(8)
$N=4$	-2.95040		
$N=5$	-2.90081		
$N=6$	-2.86634		
$N=7$	-2.84091		
$N=8$	-2.82133		
$N=9$	-2.80578		
$N=\infty$	-2.66667	0	21.0552

$(1,1)$ *system:* The eigenenergies of the harmonically trapped $(1,1)$ system can be obtained for any γ by solving a simple transcendental equation [21]. Expanding the transcendental equation around the known eigenenergies for small and large γ, one obtains power series in the interaction energy. Inverting these series, one obtains analytical expressions for the $B^{(k)}(1)$ and $C^{(k)}(1)$ coefficients. We find $B^{(1)}(1) = \pi^{-3/2}$, $B^{(2)}(1) = -\ln(2)/\pi^3$, $B^{(3)}(1) = -[\pi^2 - 9\ln(4)^2]/(24\pi^{9/2})$, $C^{(1)}(1) = -2\pi^{1/2}$, $C^{(2)}(1) = -4\pi[\ln(2) - 1]$, and $C^{(3)}(1) = \pi^{3/2}[\pi^2 - 24 - 9(\ln(4) - 4)\ln(4)]/3$. The numerical values of these coefficients are summarized in Tables I-II. As in the $N \to \infty$ case, the small and large γ series for $N = 1$, Eqs. (7) and (8), have a finite radius of convergence. Employing the techniques of Ref. [29], we find—using up to 50 expansion coefficients—that the small and large γ series converge for $\gamma < 1.0745(2) \times 2\pi$ and $\gamma^{-1} < [1.0745(2) \times 2\pi]^{-1}$, respectively. Our result for the convergence of the small γ series is consistent with what is reported in the literature [30].

Weakly-repulsive $(N, 1)$ system, $N = 2, 3, \cdots$: To treat

the weakly-interacting system with finite N, $N > 1$, we rewrite the system Hamiltonian in second quantization and expand the field operators for the majority particles and the impurity in terms of single particle harmonic oscillator states (see, e.g., Ref. [31]). The interaction matrix elements can be evaluated analytically and the first-order perturbation theory treatment for positive g yields

$$B^{(1)}(N) = \frac{2\sqrt{N}\Gamma(1/2 + N)}{\pi^2 N!}. \qquad (12)$$

The first-order energy shift may be interpreted as the leading-order mean-field shift. We find $\lim_{N\to\infty} B^{(1)}(N) = 2/\pi^2$, which agrees with the coefficient obtained by expanding Eq. (11). The evaluation of the second-order energy shift involves the evaluation of infinite sums. We find, as expected, that these sums converge. The reason is that the one-dimensional delta-function interaction does not, unlike two- or three-dimensional delta-function interactions [32, 33], require any regularization if used in standard perturbation theory approaches. We did not find a compact analytical expression applicable to all N for the second-order energy shift. For $N = 1$ and 2, we have $B^{(2)}(1) = -\ln(2)/\pi^3$ and $B^{(2)}(2) = [-9 + 6\sqrt{3} + 3\ln(2 + \sqrt{3}) - 12\ln(2)]/(4\pi^3)$. For larger N, the expressions are lengthy. The numerical values for $N \leq 12$ are listed in Table I. Table I also summarizes the numerically determined values for the third-order coefficients $B^{(3)}(N)$ for $N = 2 - 6$. The $B^{(3)}(N)$ coefficient increases slightly as N changes from 1 to 2, and then decreases monotonically as N increases further. The numerically determined $B^{(3)}(N)$ coefficients for $N = 2 - 6$ approach the $N = \infty$ coefficient smoothly if plotted as a function of $1/N$.

Strongly-interacting $(N, 1)$ *system, $N = 2, 3, \cdots$:* The strongly-interacting regime has been treated perturbatively at leading order, i.e., at order $1/\gamma$, for $N \leq 8$ [26] (note, though, that only the coefficients for $N \leq 4$ were reported explicitly, i.e., in equation or numerical form). To derive these results, the two-body interaction for large $|g|$ is modeled by imposing the two-body boundary condition on the many-body wave function when the distance between the unlike particles approaches zero [23, 26, 34]. Since the ground state eigenenergy for $|g| = \infty$ is degenerate, the perturbation shift is obtained by diagonalizing the perturbation matrix constructed using the degenerate states for $g = \infty$. For the many-body states Ψ_α and Ψ_β, the perturbation matrix element $V_{\alpha\beta}$ reads [23]

$$V_{\alpha\beta} = -\frac{\hbar^4}{m^2 g} \times$$

$$\sum_{j=1}^{N} \int \cdots \int \left(\left.\frac{\partial\Psi_\alpha^*}{\partial z_{j0}}\right|_{z_{j0}\to 0^+} - \left.\frac{\partial\Psi_\alpha^*}{\partial z_{j0}}\right|_{z_{j0}\to 0^-} \right) \delta(z_{j0}) \times$$

$$\left(\left.\frac{\partial\Psi_\beta}{\partial z_{j0}}\right|_{z_{j0}\to 0^+} - \left.\frac{\partial\Psi_\beta}{\partial z_{j0}}\right|_{z_{j0}\to 0^-} \right) \mathrm{d}z_0 \mathrm{d}z_1 \cdots \mathrm{d}z_N \quad (13)$$

These matrix elements are closely related to the boundary condition representation of the one-dimensional odd-parity pseudo-potential [35, 36]. We evaluate the integrals in Eq. (13) analytically for $N = 1 - 4$. The analytical results for $N = 1$ and 2 read $C^{(1)}(1) = -2\sqrt{\pi}$ and $C^{(1)}(2) = -\sqrt{\pi/2}(81/32)$. The analytical expressions for $N = 3$ and 4 are lengthy and not reported here [37]. For larger N, we perform all but one integration for each of the perturbation matrix elements analytically. The resulting numerically determined energy shifts are accurate to more than 10 digits. Table II summarizes the numerical values for the coefficient $C^{(1)}(N)$ for $N \leq 9$ obtained by us. The extension to larger N is, although tedious, possible in principle.

To determine the energy shift proportional to γ^{-2}, we use second-order perturbation theory. Reference [38] pointed out that the second-order perturbation theory energy shift of the $(1, 1)$ system diverges, thus requiring regularization. Analogous divergencies arise in the perturbative treatment of one-dimensional single-component Fermi gases with delta-prime or delta-double-prime interactions (see, e.g., Ref. [35]) and that of one-dimensional Bose gases with effective range dependent zero-range interactions. In the following, we discuss the impurity problem with $N = 2$ and 3. To evaluate the second-order energy shifts, we need to know the complete set of eigenstates of the $(2, 1)$ and $(3, 1)$ systems with $|g| = \infty$. For the $(2, 1)$ system, we use the analytical wave functions from Ref. [39] and evaluate the integrals analytically. For the $(3, 1)$ system, we derive compact forms for the eigenstates using spherical coordinates and evaluate the relevant integrals analytically. We then evaluate the second-order perturbation theory sums numerically, imposing an energy cutoff on the relative energy of the intermediate (or virtual) states that are being summed over. The second-order energy shift is found to contain powerlaw divergencies in the energy cutoff. These divergencies are canceled through the introduction of a counterterm and the constant (and physically meaningful) part is extracted with high precision by a regularization scheme similar to that developed for harmonically trapped bosons [40]. Table II reports the resulting second-order perturbation theory coefficients with errorbars. Our perturbative coefficients are consistent with the coefficients obtained by fitting the $(2, 1)$ and $(3, 1)$ energies reported in Refs. [14, 22] to a polynomial in γ^{-1}. For the $N = 2$ and 3 systems, we extend the above treatment to the third order (see Table II). These third-order calculations require the evaluation of matrix elements $V_{\alpha\beta}$ between excited states. Since the third-order perturbation expression is more involved than the second-order perturbation expression, our third-order result has a larger errorbar than our second-order result [41].

The calculations of the second- and third-order energy shifts can, in principle, be extended to larger N. To do so, two challenges need to be overcome. First, an efficient method to generate the complete set of eigenstates at $|g| = \infty$ has to be devised. Second, an efficient scheme for

TABLE III: Fitting coefficients $b_j^{(k)}$ for $k = 2$ and 3. For $k = 2$ and 3, we used $j_{max} = 6$ and 4, respectively.

	$k = 2$	$k = 3$
$j=0$	-0.0253304	1.71100×10^{-3}
$j=1$	0.0019591	2.23905×10^{-4}
$j=2$	0.0033477	6.59881×10^{-6}
$j=3$	-0.0116972	-3.67025×10^{-4}
$j=4$	0.0379414	2.64073×10^{-4}
$j=5$	-0.0684440	
$j=6$	0.0486346	

evaluating the matrix elements and infinite perturbation theory sums has to be developed. This is not pursued here.

IV. FITTING THE $B^{(k)}(N)$ AND $C^{(k)}(N)$ COEFFICIENTS

Tables I-II suggest that the coefficients $B^{(k)}(N)$ and $C^{(k)}(N)$ change, for fixed k, smoothly with N. This motivates us to write

$$B^{(k)}(N) = \sum_{j=0}^{j_{max}} b_j^{(k)} \left(\frac{1}{N}\right)^j \tag{14}$$

and

$$C^{(k)}(N) = \sum_{j=0}^{j_{max}} c_j^{(k)} \left(\frac{1}{N}\right)^j. \tag{15}$$

It should be noted that the expressions (14)-(15) reduce to $b_0^{(k)}$ and $c_0^{(k)}$, respectively, in the $N \to \infty$ limit. In the following, the parameters $b_j^{(k)}$ and $c_j^{(k)}$ are obtained by fitting the coefficients $B^{(k)}(N)$ and $C^{(k)}(N)$ for fixed k.

We start with $B^{(2)}(N)$. We fit Eq. (14) to the $B^{(2)}(N)$ values for $N = 1 - 80$ (the values for $N = 1 - 12$ are reported in Table II), varying j_{max} from $2 - 20$. We find that the most reliable fit is obtained for $j_{max} = 12 - 13$. In this case, the fitting parameter $b_0^{(2)}$ differs from $-1/(4\pi^2)$ [the result obtained by expanding Eq. (11)] by less than 10^{-8}. This suggests that not only the $k = 1$ coefficient (see discussion above) but also the $k = 2$ coefficient connects smoothly with the infinite N result. Table III reports the results of our fit to the $B^{(2)}(N)$ coefficients with $N = 1 - 80$ and ∞ by a polynomial with $j_{max} = 6$.

As mentioned earlier, the $B^{(3)}(1)$ coefficient is slightly smaller than the $B^{(3)}(2)$ coefficient. The $B^{(3)}(N)$ coefficients for $N \geq 2$, however, decrease monotonically. This motivates us to fit the $B^{(3)}(N)$ coefficients with $N = 2 - 6$ and ∞ by a polynomial with $j_{max} = 4$. The fit coefficients are reported in Table III. It can be seen that the coefficient $b_0^{(3)}$ agrees with the coefficient $B^{(3)}(\infty)$ reported in Table I. We believe that our fit provides an accurate description of the $6 < N < \infty$ coefficients.
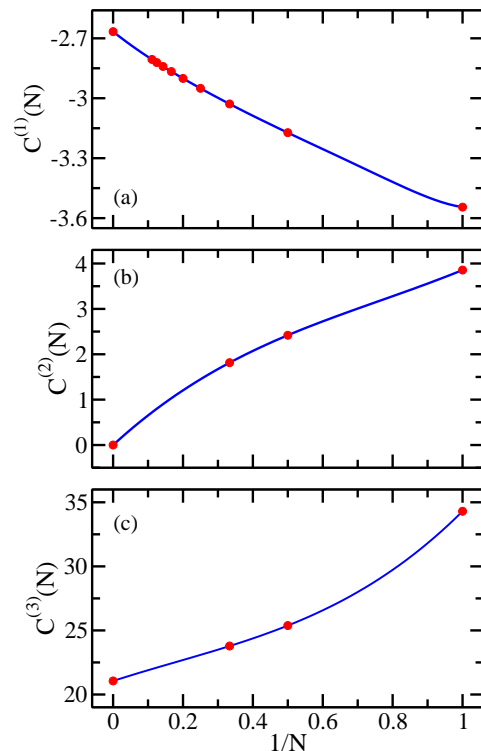

FIG. 2: (Color online) Symbols show the coefficients (a) $C^{(1)}(N)$, (b) $C^{(2)}(N)$, and (c) $C^{(3)}(N)$ as a function of $1/N$. The solid lines show our fits with $j_{max} = 6, 3$, and 3, respectively.

TABLE IV: Fitting coefficients $c_j^{(k)}$ for $k = 1, 2$, and 3. For $k = 1, 2$, and 3, we used $j_{max} = 6, 3$, and 3, respectively.

	$k = 1$	$k = 2$	$k = 3$
$j=0$	-2.66667	0.00000	21.05520
$j=1$	-1.40749	7.06739	8.80915
$j=2$	1.78704	-5.70589	-5.07455
$j=3$	-4.21746	2.49453	9.51090
$j=4$	7.33094		
$j=5$	-7.13604		
$j=6$	2.76476		

Symbols in Figs. 2(a)-2(c) show the $C^{(k)}(N)$ coefficients with $k = 1, 2$, and 3, respectively, as a function of $1/N$. Our fits to these data (see Table II) using polynomials with $j_{max} = 6, 3$, and 3 are shown by solid lines (see Table IV for the coefficients).

The discussion so far has focused on the coefficients $B^{(k)}(N)$ and $C^{(k)}(N)$ with $k = 1-3$. It is, in general, not feasible to extend the perturbative calculations to higher k for arbitrary N. However, for $N = 1$ and ∞, the coefficients with larger k can be obtained readily. We find that $|B^{(k)}(1)|$ decreases monotonically with increasing k (we checked this for $k \leq 50$). The $|C^{(k)}(1)|$ coefficient

increases monotonically with increasing k for $k < 37$; for $k \geq 37$, we observe small non-monotonic oscillations. For $N = \infty$, we find that the $B^{(k)}(\infty)$ with k even and $k \geq 4$ vanish while the $|B^{(k)}(\infty)|$ with k odd decrease monotonically with increasing k (again, we checked this for $k \leq 50$). Similarly, the $C^{(k)}(\infty)$ with k even and $k \geq 2$ vanish while the $|C^{(k)}(\infty)|$ with k odd increase monotonically with increasing k. Assuming a linear change with $1/N$, interpolating between $B^{(k)}(1)$ and $B^{(k)}(\infty)$ and between $C^{(k)}(1)$ and $C^{(k)}(\infty)$ for $k > 3$ yields estimates for the finite N, $N > 1$, coefficients. While rough, these estimates might provide a reasonable means to connect the weak and strong perturbation theory limits for quantities such as those shown in Figs. 3 and 4.

We cannot accurately estimate the radius of convergence of the small and large γ expansions for $1 < N < \infty$. However, the fact that the radius of convergence is given by $\gamma < 1.0745(2) \times 2\pi$ for $N = 1$ and $\gamma < 2\pi$ for $N = \infty$ for the small γ series and by $\gamma^{-1} < [1.0745(2) \times 2\pi]^{-1}$ for $N = 1$ and $\gamma^{-1} < (2\pi)^{-1}$ for $N = \infty$ for the large γ series suggests two speculations: First, a convergent series can be found for any γ and N. Second, the radius of convergence of the small γ series is approximately 2π for all N. Figures 3 and 4, which are discussed in the next section, are consistent with these speculations.

V. DISCUSSION

This section compares the perturbative energy expressions with the numerically determined energies of the upper branch. Figure 1(b) shows that the scaled interaction energy $\epsilon(N)/E_\mathrm{F}(N)$ depends weakly on N if plotted as a function of $-\hbar\omega a_\mathrm{ho}/g$. The dependence on N is even weaker when the interaction strength is parameterized by γ as opposed to g. To benchmark the applicability of the perturbative expressions we analyze the interaction energy of the system with N majority atoms by comparing with that of the $(1,1)$ system. Specifically, we consider the quantities $\rho(N)$,

$$\rho(N) = \frac{\epsilon(N)/E_\mathrm{F}(N)}{\epsilon(1)/E_\mathrm{F}(1)}, \qquad (16)$$

and $\delta(N, N')$,

$$\delta(N, N') = \frac{\epsilon(N)/E_\mathrm{F}(N) - \epsilon(1)/E_\mathrm{F}(1)}{\epsilon(N')/E_\mathrm{F}(N') - \epsilon(1)/E_\mathrm{F}(1)}. \qquad (17)$$

For finite N, $\rho(N)$ reduces to $\epsilon(N)/[N\epsilon(1)]$, i.e., $\rho(N)$ tells one the interaction energy per particle, normalized by the interaction energy of the $(1,1)$ system. The quantity $\delta(N, N')$ can alternatively be written as $[\rho(N) - 1]/[\rho(N') - 1]$.

Expanding Eq. (16) in the weakly-interacting (small γ) regime, we find

$$\rho(N) = \rho_0^{(\mathrm{w})}(N) + \rho_1^{(\mathrm{w})}(N)\gamma + \rho_2^{(\mathrm{w})}(N)\gamma^2 + \mathcal{O}(\gamma^3), (18)$$
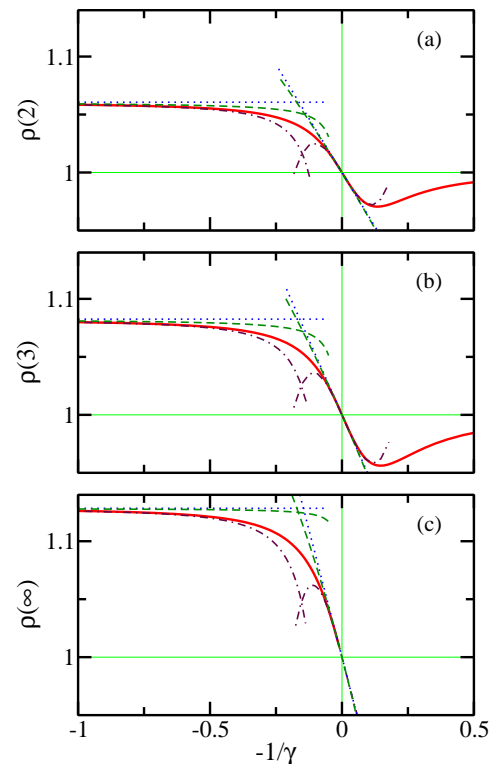

FIG. 3: (Color online) Solid lines show the quantity $\rho(N)$ as a function of $-1/\gamma$ for (a) $N = 2$, (b) $N = 3$, and (c) $N = \infty$, respectively. For comparison, dotted, dashed, and dash-dotted lines show the perturbative results for $\rho(N)$ accounting for terms up to order γ^0, γ^1 and γ^2, respectively, in the weakly-interacting regime and accounting for terms up to order γ^{-1}, γ^{-2} and γ^{-3}, respectively, in the strongly-interacting regime.

where the coefficients $\rho_k^{(\mathrm{w})}(N)$ are determined by the $B^{(l)}(N)$ and $B^{(l)}(1)$ with $l \leq k + 1$. Expanding Eq. (16) in the strongly-interacting (large $|\gamma|$) regime, we find

$$\rho(N) = 1 + \rho_1^{(\mathrm{s})}(N)\gamma^{-1} + \rho_2^{(\mathrm{s})}(N)\gamma^{-2} + \rho_3^{(\mathrm{s})}(N)\gamma^{-3} + \mathcal{O}(\gamma^{-4}), \qquad (19)$$

where the coefficients $\rho_k^{(\mathrm{s})}(N)$ are determined by the $C^{(l)}(N)$ and $C^{(l)}(1)$ with $l \leq k$. Solid lines in Figs. 3(a)-3(c) show the quantity $\rho(N)$ for $N = 2$, 3, and ∞, respectively. The solid lines are obtained using the numerical $(2,1)$ and $(3,1)$ energies and the semi-analytical $(1,1)$ and $(\infty,1)$ energies. For $\gamma \to 0^+$ (i.e., for $-1/\gamma \to -\infty$), the quantity $\rho(N)$ approaches the constant $\rho_0^{(\mathrm{w})}(N) = B^{(1)}(N)/B^{(1)}(1)$ [see the horizontal dotted lines in Figs. 3(a)-3(c)], which increases monotonically from 1.0607 to 1.1284 as N goes from 2 to ∞. This portion of the interaction energy can be interpreted as the mean-field contribution. Inclusion of the next order correction [the $\rho_1^{(\mathrm{w})}(N)\gamma$ term] and the next two corrections

[the $\rho_1^{(w)}(N)\gamma$ and $\rho_2^{(w)}(N)\gamma^2$ terms] yields the dashed and dash-dotted lines in Figs. 3(a)-3(c). The dash-dotted lines provide a fairly accurate description of the quantity $\rho(N)$ for $-1/\gamma \lesssim -0.4$. For $|\gamma| \to \infty$, the leading-order γ-dependent term [see the (non-horizontal) dotted lines in Figs. 3(a)-3(c)] increases monotonically from 0.3725 to 0.8782 as N changes from 2 to ∞. Inclusion of the next-order correction and the next two corrections yields the dashed and dash-dotted lines in Figs. 3(a)-3(c). It can be seen that the dash-dotted lines provide a fairly accurate description of the quantity $\rho(N)$ for $-1/\gamma \gtrsim -0.15$. This value is close to the expected radius of convergence of the interaction energy [recall, the radius of convergence is $1/\gamma = (1.0745 \times 2\pi)^{-1} \approx 0.148$ for the $(1,1)$ system]. Combining the perturbative descriptions for small and large $|\gamma|$, the expansions provide a fairly accurate description of the interaction energy for the system with N majority particles, normalized by that for the $(1,1)$ system, over a wide range of interaction strengths γ.

Expanding Eq. (17) in the weakly-interacting regime, we find

$$\delta(N,N') = \delta_0^{(w)}(N,N') + \delta_1^{(w)}(N,N')\gamma +$$
$$\delta_2^{(w)}(N,N')\gamma^2 + \mathcal{O}(\gamma^3), \qquad (20)$$

where the coefficients $\delta_k^{(w)}(N,N')$ are determined by the $B^{(l)}(N)$, $B^{(l)}(N')$, and $B^{(l)}(1)$ with $l \leq k+1$. Expanding Eq. (17) in the strongly-interacting regime, we find

$$\delta(N,N') = \delta_0^{(s)}(N,N') + \delta_1^{(s)}(N,N')\gamma^{-1} +$$
$$\delta_2^{(s)}(N,N')\gamma^{-2} + \mathcal{O}(\gamma^{-3}), \qquad (21)$$

where the coefficients $\delta_k^{(s)}(N,N')$ are determined by the $C^{(l)}(N)$, $C^{(l)}(N')$, and $C^{(l)}(1)$ with $l \leq k+1$. The quantity $\delta(N,N')$ is shown by the solid line in Fig. 4(a) for $(N,N') = (2,\infty)$ and by dots in Figs. 4(b)-4(c) for $(3,\infty)$ and $(2,3)$, respectively. We observe that the quantity $\delta(N,N')$ changes only slightly as $-1/\gamma$ goes from $-\infty$ to 0; this is particularly true for $\delta(2,3)$ [see Fig. 4(c)]. The limiting values [see the dotted lines in Figs. 4(a)-4(c)] are given by $\delta_0^{(w)}(N,N')$ and $\delta_0^{(s)}(N,N')$, respectively. Dashed lines include the next order correction in the weakly- and strongly-interacting regimes, and dash-dotted lines include the next two corrections. In the weakly-interacting regime, the dash-dotted lines provide a fairly good description of the quantity $\delta(N,N')$. In the strongly-interacting regime, however, the validity regime of the perturbative expressions is quite small. For $\delta(2,3)$, e.g., the expansion coefficients are $\delta_0^{(s)}(2,3) = 0.7213$, $\delta_1^{(s)}(2,3) = 0.0694(3)$, and $\delta_2^{(s)}(2,3) = -2.31(12)$, where the numbers in brackets denote the errorbars due to the uncertainties of the second- and third-order perturbation theory coefficients. The fact that $|\delta_2^{(s)}(2,3)| \gg |\delta_1^{(s)}(2,3)|$ is responsible for the turn-around of the dash-dotted line for large positive γ. We note that the errorbar of the quantities $\delta(3,\infty)$ and $\delta(2,3)$, obtained from the numerical energies [see dots in Figs. 4(b)-4(c)], is too large in
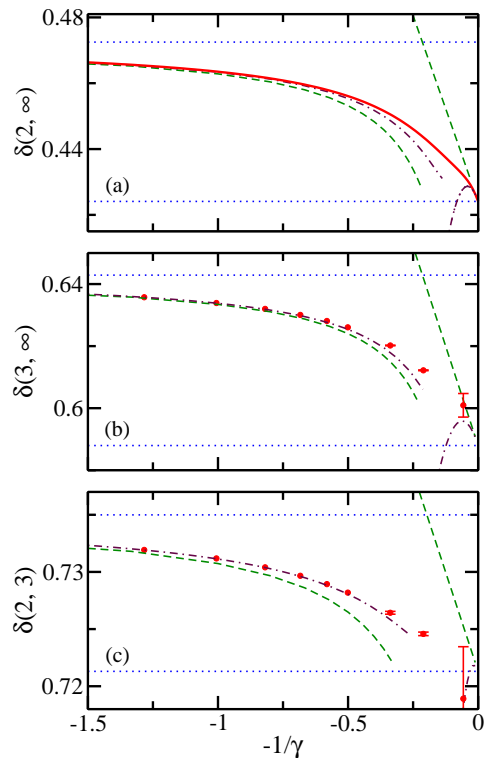

FIG. 4: (Color online) The quantity $\delta(N,N')$ as a function of $-1/\gamma$. The solid line is for (a) $N = 2$ and $N' = \infty$ and the circles are for (b) $N = 3$ and $N' = \infty$ and (c) $N = 2$ and $N' = 3$. In the large γ regime, the uncertainty of the numerically determined $(3,1)$ energies leads to appreciable uncertainties in $\delta(2,3)$ and $\delta(3,\infty)$ [see the errorbars in Figs. 4(b) and 4(c)]. For comparison, dotted, dashed, and dash-dotted lines show the perturbative results for $\delta(N,N')$ accounting for terms up to order γ^0, γ^1, and γ^2, respectively, in the weakly-interacting, small $|\gamma|$ regime and accounting for terms up to order γ^{-1}, γ^{-2}, and γ^{-3}, respectively, in the strongly-interacting, large $|\gamma|$ regime.

the large γ regime to meaningfully compare with the perturbative results.

VI. CONCLUSION

This paper considered the upper branch of a non-interacting harmonically trapped one-dimensional Fermi gas with a single impurity. Zero-range two-body contact interactions with strength g were assumed between the majority atoms and the impurity. This system constitutes one of the simplest mesoscopic systems accessible to experiment and theory. On the experimental side, it has been demonstrated by the Heidelberg group that the upper branch of the model Hamiltonian can be emulated reliably using ultracold atoms [18, 19]. On the theory

side, various numerical and analytical techniques have been applied [7, 11–17, 23–26]. This paper pursued a perturbative approach, which determined expansions of the energy of the upper branch in the weakly- and strongly-interacting regimes for various N. In the cases where we were not able to obtain general N expressions for a fixed order in the perturbative expansion, approximate expressions applicable to all N were obtained through fits. Through comparison with accurate numerical few-body energies, the perturbative expressions were shown to provide a satisfactory description for a wide range of interaction strengths.

The main results of this work are: (i) We determined an expansion for the energy of the upper branch of a one-dimensional harmonically trapped Fermi gas with a single impurity in the weakly-repulsive regime up to order γ^3, applicable to any system size. (ii) We determined an expansion for the energy of the upper branch in the strongly-interacting regime up to order γ^{-3}, applicable to any system size. While the idea to treat the coupling strength $1/\gamma$ as a small parameter is not new, our work provides an explicit demonstration that such a program can be carried through explicitly beyond the leading-order correction. (iii) The radii of convergence of the series were reported for $N = 1$ and ∞. (iv) The behavior of the expansion coefficients in the series in γ^k and γ^{-k} with $k > 3$ was discussed. (v) The perturbative expressions were benchmarked and found to provide a reliable description over a wide range of interaction strengths.

The results presented in this work can be used to calculate perturbative expressions for the contact and other observables. Moreover, the second- and third-order results in the γ^{-1} series allow one to assess the applicability regime of effective spin models [26, 34, 42].

[1] D. C. Mattis, *The Many-Body Problem. An Encyclopedia of Exactly Solved Models in One Dimension*, World Scientific, 1993.

[2] T. Giamarchi, *Quantum Physics in One Dimension*, Oxford University Press, Oxford, 2004.

[3] A. Imambekov, T. L. Schmidt, and L. I. Glazman, Rev. Mod. Phys. **84**, 1253 (2012).

[4] X.-W. Guan, M. T. Batchelor, and C. Lee, Rev. Mod. Phys. **85**, 1633 (2013).

[5] Z. N. C. Ha. *Quantum Many-Body Systems in One Dimension*, Series on Advances in Statistical Mechanics - Volume 12, World Scientific, 1996.

[6] C. Menotti and S. Stringari, Phys. Rev. A **66**, 043610 (2002).

[7] G. E. Astrakharchik and I. Brouzos, Phys. Rev. A **88**, 021602(R) (2013).

[8] G. E. Astrakharchik, D. Blume, S. Giorgini, and L. P. Pitaevskii, Phys. Rev. Lett. **93**, 050402 (2004).

[9] I. V. Tokatly, Phys. Rev. Lett. **93**, 090405 (2004).

[10] G. Orso, Phys. Rev. Lett. **98**, 070402 (2007).

[11] M. Casula, D. M. Ceperley, and E. J. Mueller, Phys. Rev. A **78**, 033607 (2008).

[12] I. Brouzos and P. Schmelcher, Phys. Rev. A **87**, 023605 (2013).

[13] N. L. Harshman, Phys. Rev. A **86**, 052122 (2012).

[14] S. E. Gharashi, K. M. Daily, and D. Blume, Phys. Rev. A **86**, 042702 (2012).

[15] S. E. Gharashi and D. Blume, Phys. Rev. Lett. **111**, 045302 (2013).

[16] P. O. Bugnion and G. J. Conduit, Phys. Rev. A **87**, 060502(R) (2013).

[17] T. Sowiński, T. Grass, O. Dutta, and M. Lewenstein, Phys. Rev. A **88**, 033607 (2013).

[18] F. Serwane, G. Zürn, T. Lompe, T. B. Ottenstein, A. N. Wenz, and S. Jochim, Science **332**, 6027 (2011).

[19] A. N. Wenz, G. Zürn, S. Murmann, I. Brouzos, T. Lompe, and S. Jochim, Science **342**, 457 (2013).

[20] M. Olshanii, Phys. Rev. Lett. **81**, 938 (1998).

[21] T. Busch, B.-G. Englert, K. Rzążewski, and M. Wilkens, Found. Phys. **28**, 549 (1998).

[22] In the vicinity of $|g| \to \infty$, we improved the numerical energies reported in Ref. [15].

[23] A. G. Volosniev, D. V. Fedorov, A. S. Jensen, M. Valiente, and N. T. Zinner, Nat. Commun. **5**, 5300 (2014).

[24] E. J. Lindgren, J. Rotureau, C. Forssén, A. G. Volosniev, and N. T. Zinner, New J. Phys. **16**, 063003 (2014).

[25] X. Cui and T.-L. Ho, Phys. Rev. A **89**, 023611 (2014).

[26] J. Levinsen, P. Massignan, G. M. Bruun, and M. M. Parish, arXiv:1408.7096.

[27] Throughout, we refer to the expansion around $\gamma = 0^+$ and $|\gamma^{-1}| = 0$ as small and large γ series. Sections III and IV discuss the applicability regime, i.e., the radius of convergence, of these series.

[28] J. B. McGuire, J. Math. Phys. **6**, 432 (1965).

[29] J. Zamastil and F. Vinette, J. Phys. A: Math. Gen. **38**, 4009 (2005).

[30] S. Kvaal, E. Jarlebring, and W. Michiels, Phys. Rev. A **83**, 032505 (2011). Converted to our units, this reference reports that the small γ series converges for $\gamma < 2\pi$. Inspection of the inset of Fig. 2 of this reference suggests, however, that the radius of convergence is slightly larger than 2π.

[31] A. J. Leggett, *Quantum Liquids: Bose Condensation and Cooper Pairing in Condensed-Matter Systems*, Oxford University Press Inc., New York, 2006.

[32] K. Huang and C. N. Yang, Phys. Rev. **105**, 767 (1957).

[33] K. Wódkiewicz, Phys. Rev. A **43**, 68 (1991).

[34] F. Deuretzbacher, D. Becker, J. Bjerlin, S. M. Reimann, and L. Santos. Phys. Rev. A **90**, 013611 (2014).

[35] M. D. Girardeau and M. Olshanii, Phys. Rev. A **70**,

023608 (2004).

[36] T. Cheon and T. Shigehara, Phys. Rev. Lett. **82**, 2536 (1999).

[37] Our $C^{(1)}(3)$ coefficient agrees with that reported in Ref. [26] but differs by 0.0012 % from the slope that one obtains using the adiabatic wave function reported in Ref. [15] [see Eq. (2) of the supplemental material]. This implies (see also Ref. [26]) that the true adiabatic wave functions are linear combinations of Eqs. (2) and (3) of the supplemental material of Ref. [15] with coefficients $\alpha \approx 0.9999929$ and $-(1 - \alpha^2)^{1/2} \approx -0.003764883$ for state 1 and coefficients $(1 - \alpha^2)^{1/2}$ and α for state 2. An analogous analysis shows that the true adiabatic wave functions of the $(2,2)$ system are linear combinations of Eqs. (11) and (12) of the supplemental material of Ref. [15] with coefficients $-(1 - \alpha^2)^{1/2}$ and α for the state with larger slope and α and $(1 - \alpha^2)^{1/2}$ for the state with smaller slope. Lastly, the perturbation analysis allows one to improve the accuracy of the coefficient $c^2 = 0.865(7)$, which is reported below Eq. (10) of the supplemental material of Ref. [15]; the perturbative analysis yields $c^2 \approx 0.8626961$.

[38] D. Sen, Int. J. Mod. Phys. A **14** 1789 (1999).

[39] A. G. Volosniev, D. V. Fedorov, A. S. Jensen, and N. T. Zinner, arXiv:1408.6058.

[40] P. R. Johnson, D. Blume, X. Y. Yin, W. F. Flynn, and E. Tiesinga, New J. Phys. **14**, 053037 (2012).

[41] For the $N = 2$ system, we used energy cutoffs of $1920\hbar\omega$ and $708\hbar\omega$ for the second- and third-order perturbation theory calculations. For the $N = 3$ system, we used energy cutoffs of $190\hbar\omega$ and $80\hbar\omega$ for the second- and third-order perturbation theory calculations.

[42] A. G. Volosniev, D. Petrosyan, M. Valiente, D. V. Fedorov, A. S. Jensen, and N. T. Zinner. arXiv:1408.3414.